Immunosubunit β5i Knockout Suppresses Neovascularization and Restores Autophagy in Retinal Neovascularization by Targeting ATG5 for Degradation

Liyang Ji,[2] Li Li,[4] Ying Zhao,[5] Shengqiang Liu,[1] Jingmin Li,[1] Jinsong Zhang,[2,3] Qi Zhao,[1] and Shuai Wang[1]

[1]Department of Ophthalmology, The Second Affiliated Hospital of Dalian Medical University, Dalian, China
[2]Department of Ophthalmology, The Fourth Affiliated Hospital of China Medical University, Shenyang, China
[3]Aier Excellence Eye Hospital, Shenyang, China
[4]Department of Ophthalmology, Zaozhuang Municipal Hospital, Zaozhuang, Shandong, China
[5]Department of Ophthalmology, Jianping County Hospital, Chaoyang, China

Correspondence: Shuai Wang, Department of Ophthalmology, The Second Affiliated Hospital of Dalian Medical University, Dalian 116000, China;
doceyewang@163.com.

Received: May 7, 2020
Accepted: November 29, 2020
Published: December 28, 2020

Citation: Ji L, Li L, Zhao Y, et al. Immunosubunit β5i knockout suppresses neovascularization and restores autophagy in retinal neovascularization by targeting ATG5 for degradation. *Invest Ophthalmol Vis Sci.* 2020;61(14):30. https://doi.org/10.1167/iovs.61.14.30

Purpose. To investigate the functional role of immunoproteasome subunit β5i in pathologic retinal neovascularization (RNV) and its ability to link the immunoproteasome and autophagy.

Methods. Oxygen-induced retinopathy (OIR) was induced in wild-type (WT) and β5i knockout (KO) mouse pups on a C57BL/6J background. Proteasome catalytic subunit expression and proteasome activity were evaluated by quantitative real-time PCR (qPCR) and proteasome activity. Retinal vascular anatomy and neovascularization were characterized and quantified by retinal vascular flat-mount staining, fluorescence angiography, platelet endothelial cell adhesion molecule (PECAM) immunostaining, and hematoxylin and eosin staining. Correlation factors, including VEGF and ICAM-1, were detected by qPCR. Autophagy was examined by transmission electron microscopy (TEM). Autophagy biomarkers, including LC3, P62, ATG5, and ATG7, were measured by immunostaining and immunoblotting. The protein interaction between β5i and ATG5 was detected by immunoprecipitation.

Results. We observed that β5i had the greatest effect in WT OIR mice. Fundus fluorescence angiography, retinal flat-mount staining, and PECAM staining revealed that pathologic RNV decreased in β5i KO OIR mice compared with WT OIR mice. Concurrently, TEM, immunostaining, and immunoblotting showed that autophagy was induced in β5i KO OIR mice compared to WT OIR mice through increases in autophagosome and LC3 expression and a decrease in P62. Mechanistically, β5i interacted with ATG5 and promoted its degradation, leading to autophagy inhibition and pathogenic RNV.

Conclusions. This study identifies a functional role for β5i in RNV regulation. β5i deletion ameliorates RNV and restores autophagy by stabilizing ATG5. These results demonstrate the potential of β5i to serve as a bridge linking the immunoproteasome and autophagy.

Keywords: retinal neovascularization, immunosubunit β5i, autophagy

Retinal neovascularization (RNV) is a common pathological change that occurs in multiple ophthalmic diseases, including proliferative diabetic retinopathy,[1] retinal vein occlusion,[2] and retinopathy of prematurity.[3] The hallmarks of RNV are aberrant new vessel growth. Rapidly growing vessels have common structural abnormalities that cause these fragile immature vasculatures to hemorrhage easily.[4] Moreover, severe RNV drives proliferative membrane formation and ultimately retinal detachment, which is a major cause of vision loss.[5] Multiple biological processes, such as the unfolded protein response, oxidative stress, inflammation, autophagy, and pyroptosis, have been demonstrated to play a role in the pathological conditions of RNV.[6–8] These interrelated phenomena all modulate the pathological RNV process; however, there is limited evidence of their relationships in RNV.

To maintain cellular homeostasis, organisms have evolved several protein degradation systems to digest unfolded or unnecessary proteins. The ubiquitin–proteasome system (UPS) and autophagy are two major pathways for protein digestion.[9] The standard proteasome is comprised of three β catalytic subunits—namely, β1 (PSMB6), β2 (PSMB7), and β5 (PSMB5)—which have caspase-like, trypsin-like, and chymotrypsin-like activity, respectively.[10] When activated by cytokines, these subunits are replaced by inducible subunits, β1i (PSMB9), β2i (PSMB10), and β5i (PSMB8), to form the immunoproteasome.[11] The immunoproteasome has been reported to be involved in retinal injury, glaucoma, and hypertensive retinopathy.[12–15] Autophagy functions by removing long-lived and aggregated proteins and digesting damaged organelles.[16] It has long been reported that the UPS and autophagy show different regulatory patterns,[14,17] but

recent studies have suggested that they complement each other.[9,18] Novel therapeutic strategies based on the relationship between these systems still must be investigated. In addition, we previously found that β5i is expressed in the ganglion cell layer (GCL), inner plexiform layer (IPL), inner nuclear layer (INL), outer plexiform layer (OPL), and retinal pigment epithelium (RPE) in the retina and that deletion of β5i reduces hypertensive retinopathy.[15] We also found that autophagy is attenuated in pathologic RNV in oxygen-induced retinopathy (OIR) mice.[6] However, the role of β5i in pathologic RNV and whether it modulates autophagy remain largely unknown.

In the present study, by using an OIR model and β5i knockout (KO) mice, we found that β5i functions as a positive regulator by directly targeting ATG5 degradation. This study shows, for the first time to the best of our knowledge, that β5i has a novel role as a proangiogenic factor in pathologic RNV, which strongly indicates a compensatory effect between the UPS and autophagy in this condition.

Materials and Methods

Animal Experiments

Wild-type (WT) mice and β5i KO mice (β5i KO, STOCK Psmb8^{tm1Hjf}/J, C57BL/6J) were purchased from The Jackson Laboratory (Bar Harbor, ME, USA). The DNA of mice was isolated from the tails or fingernails and subjected to PCR analyses for genotyping. β5i KO mice were identified by PCR analysis using forward (5′-CCGACGGCGAGGATCTCGTCGTGA-3′) and reverse (5′-CTTGTACAGCAGGTCACTGACATCG-3′) primers. β5i KO mice were bred by heterozygous × heterozygous. WT and β5i KO mice were littermates with the same background in this study.[12,15] At least three litters were involved in each part of the experiments.

OIR was induced in young postnatal mice as previously described.[19] In brief, the OIR group mice and their nursing mothers were exposed to 75% ± 5% oxygen from postnatal day 7 (P7) to P12. Oxygen levels were checked using a CY-12C portable oxygen measuring instrument (AIPU Instrument, Ltd., Hangzhou, China). On P12, the mice were subsequently returned to standard housing conditions (21% oxygen) for an additional 5 days. The mice in the room air (RA) group were maintained in normal RA from birth until P17. The incubator temperature was maintained at 21°C ± 2°C with 45% to 60% humidity on a 12/12-hour day/night cycle, and food and water were available ad libitum. After we photographed the fundus at P17, we anesthetized all mice by intraperitoneal (IP) injection of an overdose of pentobarbital (100 mg/kg; Sigma-Aldrich, St. Louis, MO, USA). The eyes were prepared for further histological and molecular analyses. All animal experiments were approved by the Institutional Animal Care and Use Committee of Dalian Medical University and conformed to the ARVO Statement for the Use of Animals in Ophthalmic and Vision Research and the Guide for the Care and Use of Laboratory Animals adopted by the National Institutes of Health (No. 85–23).[20]

Histopathological Analysis

Eyes from P17 mice were quickly removed and fixed in 4% paraformaldehyde for 24 hours. After paraffin embedding, the blocks were sectioned at 5 µm. Selected sections were stained with hematoxylin and eosin (H&E) according to a standard procedure. Briefly, after they were deparaffinized and rehydrated, sections were stained in hematoxylin for 3 minutes and differentiated in 1% acid alcohol for 30 seconds. Sections were then counterstained in eosin for 30 seconds. The nuclei of new vessels extending from the retina to the vitreous were counted. Digital images of more than 10 random fields from each retinal sample were taken at 400× magnification using an Olympus fluorescence microscope (Olympus Corporation, Tokyo, Japan).

Immunostaining

Immunostaining was done as reported before.[6,15] Briefly, 5-µm-thick retina frozen sections from P17 mice were used. The eye sections were permeabilized with 0.3% Triton X-100/PBS for 30 minutes at room temperature (RT), blocked with 3% BSA/PBS, and then incubated at 4°C overnight with anti-β5i (ab3329, 1:100; Abcam, Cambridge, UK), anti-microtubule-associated protein 1 light chain 3α (LC3, ab48394, 1:500; Abcam), and anti-platelet endothelial cell adhesion molecule (PECAM) antibodies (ab24590, 1:20; Abcam) followed by Alexa Fluor 594 (ab150116) and Alexa Fluor 488 (ab150077) (1:1000; Abcam) conjugated secondary antibodies (for PECAM and for β5i and LC3, respectively) at a 1:200 dilution for 1 hour and 4′,6-diamidino-2-phenylindole (DAPI, 1:10,000; Sigma-Aldrich) for 5 minutes. Four nonoverlapping fields of each section were taken at 200× magnification after background correction and analyzed by ImageJ software (National Institutes of Health, Bethesda, MD, USA).[21] Fluorescein intensity was calculated by multiplying the positive stained area by intensity (mean) in the same area of the retina. Relative intensity was normalized to WT normoxia control mice.

Fundus Fluorescein Angiography

P17 mice were lightly anesthetized by IP injection of 2.5% tribromoethanol (0.020 mL/g; Sigma-Aldrich). Before the procedure, the eyes were dilated with one drop of tropicamide solution (Alcon, Fort Worth, TX, USA) and lubricated with hypromellose ophthalmic demulcent solution (Gonak; Akorn Pharmaceuticals, Lake Forest, IL, USA). We then placed the mice on a custom heated stage for imaging. Fundus fluorescein angiography (FFA) was performed immediately after fluorescein sodium (13 mL/kg in saline; Alcon) injection via the tail vein. Images were captured every 30 seconds for 5 minutes using a retinal imaging system (OPTO-RIS; Optoprobe Science, Burnaby, BC, Canada). Fluorescence intensity was calculated by multiplying the mean retinal vessel intensity by vessel area.[15,22] Retinal vein width for each mouse was measured by selecting two points horizontally at the edge of the vein.[23] Retinal arterial tortuosity was calculated as the ratio of actual vessel length to the straight linear length from the optic disc to the edge of FFA images.[23,24] Average retinal vein width and artery tortuosity were used to represent each mouse. All parameters were measured using ImageJ software.[25] All of the captures were normalized to the WT in RA group.

Retinal Flat-Mount Staining

For retinal flat-mount staining, eyes from P12 and P17 mice were fixed in 4% PFA for 1 hour, and retinas were then dissected out. After permeabilization with 0.5% Triton X-100/PBS for 1 hour at RT, retinas were incubated with

Investigative Ophthalmology & Visual Science

Isolectin GS-IB4 (20 µg/mL; Invitrogen, Carlsbad, CA, USA) for 2 hours at RT. After being washed in PBS, retinas were flat-mounted with 60% glycerol in PBS. Images were taken with a laser scanning confocal microscope (DMI6000B with TCS SP8 system; Leica, Wetzlar, Germany) at 10× magnification. The relative neovascular area and avascular area were analyzed with ImageJ software. The Freehand tool was used to select the edge of the retina and vaso-obliteration area. For the neovascular area, captures were inverted and shifted to 8-bit, and the threshold was set at 225. The ratios calculated were vaso-obliteration area to retina area and neovascular area to retina area.

Quantitative Real-Time PCR Analysis

Complementary DNA was generated from 1 µg of total RNA extracted from each sample at P17 according to standard methods (Promega Corporation, Madison, WI, USA). Quantitative real-time PCR (qPCR) was performed with the 7500 Fast Real-Time PCR System (Applied Biosystems, Foster City, CA, USA) at 95°C for 15 seconds, 60°C for 30 seconds, and 72°C for 30 seconds for 40 cycles and then quantified by the $2^{-\Delta\Delta CT}$ method.[26] The levels of all detected mRNAs were normalized to the level of glyceraldehyde 3-phosphate dehydrogenase (GAPDH).

Western Blot Analysis

Retinas from P17 mice were lysed with lysis buffer and then homogenized. Equal amounts of protein (30 µg) were loaded and separated on sodium dodecyl sulfate–polyacrylamide gel electrophoresis (SDS-PAGE) gels, transferred to polyvinylidene difluoride membranes, incubated with different primary antibodies, and then incubated with secondary antibody (ab7090, 1:2000; Abcam). All blots were generated by a FluorChem M system (ProteinSimple, San Jose, CA, USA) and analyzed by a Gel-Pro 4.5 Analyzer (Media Cybernetics, Rockville, MD, USA). The relative intensities were normalized to the intensity of GAPDH in each sample. The primary antibodies were as follows: β5i (ab3329, 1:1000; Abcam); vascular endothelial growth factor (VEGF, ab214424, 1:1000; Abcam); and ATG5 (12994), ATG7 (8558), LC3 (ab48394, 1:1000; Abcam), P62 (23214), protein kinase B (AKT, 9272), p-AKT (9271), p-ERK1/2 (9101), ERK1/2 (9102), and GAPDH (2118, 1:800; Cell Signaling Technology, Danvers, MA, USA).

Transmission Electron Microscope

Transmission electron microscopy (TEM) was conducted as before.[6] Eyes from P17 mice were fixed in 2.5% glutaraldehyde at 4°C overnight, incubated in 1% osmium tetroxide, dehydrated in ethanol, and embedded in gradient epoxy resin. Ultrathin sections were sliced with an MT 5000 Sorvall ultramicrotome (DuPont, Wilmington, DE, USA) and stained with 3% uranyl acetate and 3% lead citrate for 15 minutes at RT. Sections were imaged with a TEM system.

Proteasome Activity Measurement

To measure proteasome activity, retinal proteins from P17 mice were extracted in HEPES buffer (50 mM, pH 7.5; in 20-mM KCl, 5-mM $MgCl_2$, and 1-mM dithiothreitol). A total of 20 µg of protein was added to HEPES buffer containing different fluorogenic substrates, including Z-LLE-AMC (5 mmol/L), Ac-RLRAMC (40 mmol/L), and Suc-LLVY-AMC (8 mmol/L; all from Promega) for 1 hour at 37°C to detect caspase-like, trypsin-like, and chymotrypsin-like activity, respectively. We measured the fluorescence intensity at an excitation wavelength of 380 nm and an emission wavelength of 460 nm.

Immunoprecipitation

Retinas from P17 mice were lysed and homogenized in lysis buffer. Samples were then centrifuged at 12,000 rpm at 4°C for 20 minutes to obtain total protein. After quantification, 2 µg of primary antibody and Protein A-Sepharose were mixed with the protein samples, and they were shaken for 24 hours at 4°C. After washing in buffers I and II, the proteins were eluted in sample buffer. The precipitated proteins were then subjected to immunoblotting for ATG5 and β5i.

Statistical Analysis

At least three separate litters were included in each part of the present study. All results are presented as the mean ± SEM. Results were normalized to WT mice in the RA group. Data were processed using the *t*-test in two independent groups, and one-way ANOVA was used for more than two groups by using SPSS Statistics (IBM, Armonk, NY, USA). $P < 0.05$ was considered statistically significant.

Results

β5i Expression Is Upregulated in the Retinas of OIR Mice

To evaluate the immunoproteasome during pathologic RNV, we developed an OIR model and analyzed the proteasome subunits by qPCR in P17 mice. Among these subunits, β5i was the most upregulated at the mRNA level in WT OIR mice (Fig. 1A), and this was further confirmed by increased chymotrypsin-like activity (Fig. 1B). qPCR analysis also revealed that β2i mRNA expression was mildly upregulated in WT OIR mice, as confirmed by trypsin-like activity (Figs. 1A, 1B). These results were consistent with our previous findings in hypertensive retinopathy.[15] To further investigate the protein expression of β5i, we performed immunoblotting for β5i in the retinas of WT OIR mice at P17, and the results showed a corresponding change in the β5i protein expression level compared with that in the control mice (Fig. 1D). In addition, immunofluorescence showed that β5i was obviously increased in the GCL, IPL, INL, OPL, and RPE of OIR mouse retinas compared with control mouse retinas (Fig. 1C), which was also consistent with a previous study.[15] Taken together, our data reveal that β5i is a potential proangiogenic factor in the pathologic process of RNV.

β5i Deficiency Decreases Pathologic Retinal Neovascularization in OIR Mice

To document the contribution of β5i to pathologic RNV, we generated β5i deletion mice. We then induced OIR in both WT and β5i KO mice. To confirm that β5i was deleted, we examined β5i expression in the retinas of the WT mice and β5i KO mice. Immunoblotting analysis revealed that β5i was successfully deleted (Supplementary Fig. S1). To determine if β5i deletion affects retinal morphology, H&E staining

Investigative Ophthalmology & Visual Science

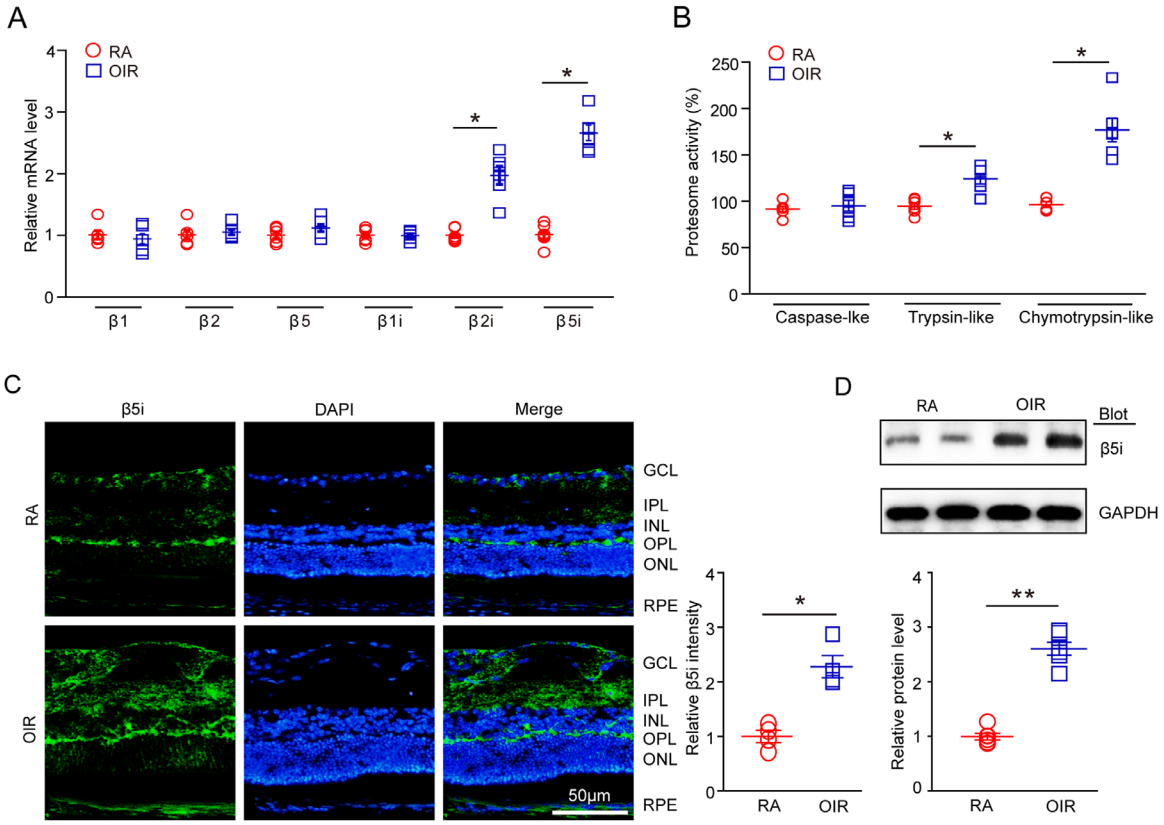

Figure 1. β5i expression is upregulated in OIR mice. (**A**) WT mice were placed in an oxygen chamber (75% ± 5% O_2) for 5 days beginning on P7 and then exposed to room air for another 5 days. qPCR was used to analyze the expression of the proteasome catalytic subunits β1, β2, β5, β1i, β2i, and β5i in retinas at P17 ($n = 6$ per group). (**B**) Proteasome activities (caspase-like, trypsin-like, and chymotrypsin-like) were measured in retinas at P17 ($n = 6$ per group). (**C**) Representative immunostaining for β5i in retinal sections from P17 mice (*left*) and quantification of the fluorescence intensity (*right*) ($n = 6$ per group). (**D**) Western blot analysis of β5i in retinas from P17 mice (*upper*) and quantification of the protein levels (*lower*) ($n = 6$ per group). Data are presented as mean ± SEM. $^{*}P < 0.05$, $^{**}P < 0.01$ versus WT normoxia controls. *Scale bars*: 50 μm.

was performed. No obvious change in retinas was observed between WT and β5i KO mice in the RA group. Endothelial cell outgrowth into the vitreous was significantly decreased in β5i KO OIR mice compared with WT OIR mice (Supplementary Fig. S2). To determine the in vivo retinal vascular response, we used FFA and retinal flat-mount staining techniques. FFA showed that β5i deletion attenuated retinal vascular intensity, retinal vein width, and retinal artery tortuosity in mice that underwent hyperoxia–hypoxia conditions compared with WT mice at P17 (Fig. 2A). Meanwhile, the neovascular area and avascular area were dramatically reduced in β5i KO OIR mice compared to WT OIR mice at P17 as determined by retinal flat-mount staining (Fig. 2B). Moreover, retinal avascular area was also decreased in β5i KO OIR mice compared with WT OIR mice at P12 (vaso-obliteration phase), which indicated that β5i deletion resulted in less vaso-obliteration, leading to less neovascularization. In addition, we observed no obvious change between WT and β5i KO mice housed under normal conditions.

To further investigate the contribution of β5i to pathologic RNV, we evaluated immunostaining for PECAM (CD31), an endothelial cell marker,[27,28] which indicated that β5i deficiency decreased retinal endothelial density in the pathologic process of RNV compared to WT OIR mice (Fig. 3A). Moreover, qPCR revealed that VEGF and ICAM-1 were upregulated in WT OIR mice compared to normal WT mice but obviously attenuated when β5i was deficient (Fig. 3B). We observed no significant differences in these parameters between the two groups when they were housed under standard conditions. Taken together, these findings indicate that ablation of β5i ameliorates pathologic RNV formation.

β5i Deletion Restores Autophagy in the Retinas of OIR Mice

An increasing number of studies have indicated that the proteasome is associated with autophagy.[9] Thus, TEM, immunostaining, and immunoblotting techniques were used to measure autophagy in retinas of WT OIR mice and β5i KO OIR mice at P17. Our previous study demonstrated that autophagy is attenuated in WT OIR mice.[6] The same results were found in the present study, confirming this phenomenon; the number of autophagosomes was decreased in the retinas of WT OIR mice compared to those of control mice. TEM also revealed that autophagy was restored in β5i KO OIR mice compared to WT OIR mice, as evidenced by an increase in the number of autophagosomes (Fig. 4A). Concurrently, retinal immunostaining of LC3, a marker of autophagy, was clearly decreased in WT OIR mice compared to WT mice but restored in β5i KO

Investigative Ophthalmology & Visual Science

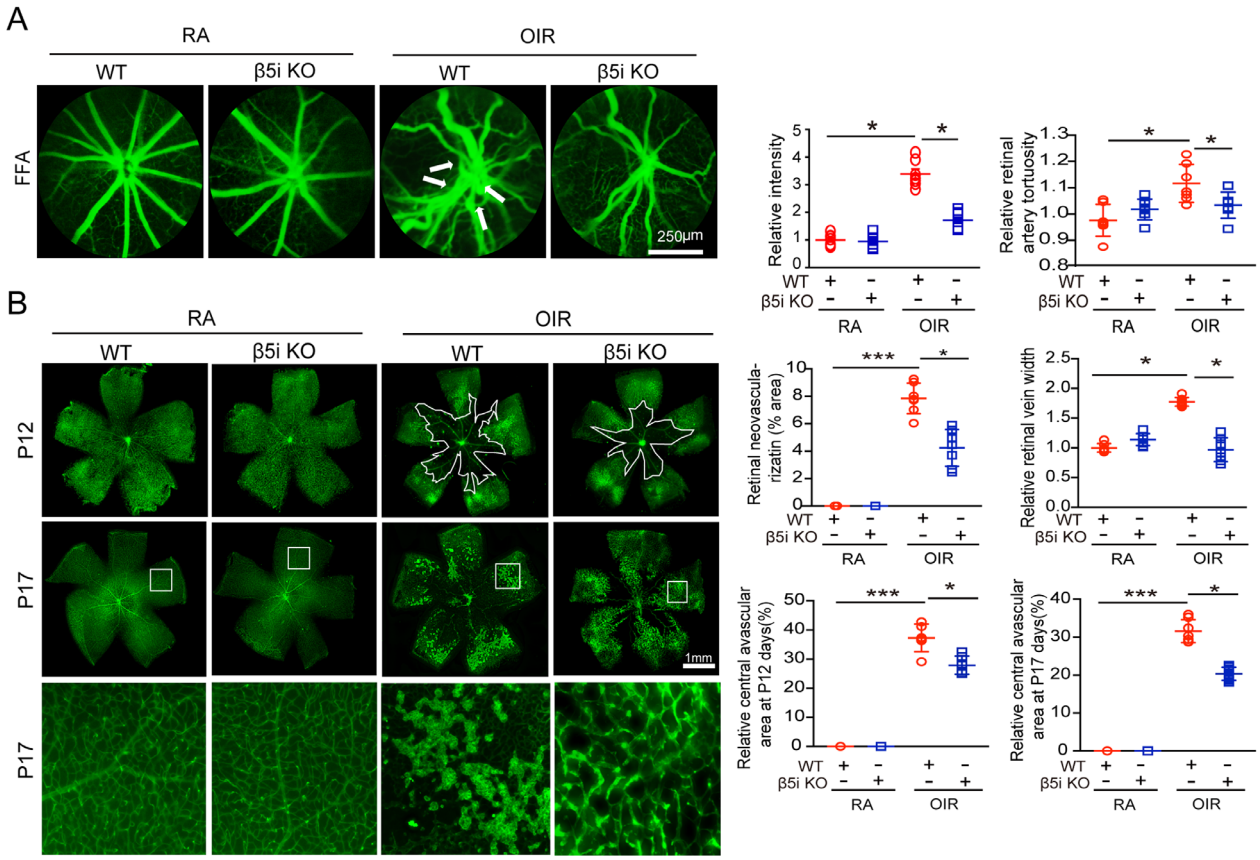

Figure 2. Genetic knockout of β5 reduces RNV. (**A**) WT and β5i KO mice were placed in an oxygen chamber (75 ± 5% O_2) for 5 days beginning on P7 and then exposed to room air for another 5 days. Representative image of FFA from P17 mice (*left*) and quantification of the relative fluorescence intensity (*right*) ($n = 7$ per group), relative retinal artery tortuosity ($n = 7$ per group), and relative retinal vein width ($n = 7$ per group). (**B**) Representative images of retinal flat-mounting staining with GSI-B4 (*left*) at P12 and P17; quantification of the neovascularization area and central avascular area at P17 (*right*) ($n = 7$ per group), as well as relative retinal central avascular area at P12 (*right*) ($n = 6$ per group). Data are presented as mean ± SEM. $^{*}P < 0.05$, $^{**}P < 0.01$, $^{***}P < 0.001$ versus WT normoxia controls. *Scale bars*: 250 μm or 1 mm.

OIR mice at P17 (Fig. 4B), suggesting that autophagy was recovered when β5i was deficient. Similarly, the LC3II/I ratio was increased at the protein level, and the expression of the autophagic substrate p62 was decreased in β5i KO OIR mice compared with WT OIR mice (Fig. 5). However, there was no obvious change in autophagy between WT and β5i KO mice housed under normal conditions. These results demonstrate that ablation of β5i functionally changes the status of autophagy in the retinas of OIR mice.

ATG5 Is Targeted by β5i in the Retinas of the OIR Model

To clarify the relationship between β5i and autophagy in the retinas of OIR mice, we immunoblotted retinal tissues from WT, β5i KO, WT OIR, and β5i KO OIR mice at P17. We analyzed the expression of autophagy-associated proteins, including ATG5 and ATG7, which are considered to play central roles in autophagy initiation. Immunoblotting analysis showed that ATG5 was upregulated in β5i KO mice compared with WT mice after exposure to hyperoxia. However, there was no significant change in ATG7 expression, which may indicate that the change in autophagy was enhanced by ATG5 (Fig. 5A). Interestingly, β5i was clearly upregulated in WT OIR mice compared to WT mice, but ATG5 was downregulated. This phenomenon, however, was completely reversed by β5i deletion, which suggested that the digestion of ATG5 by β5i might be prevented, thus restoring autophagy. To further elucidate the underlying mechanisms of the relationship between ATG5 and β5i, we examined their protein–protein interactions by immunoprecipitation. Notably, our results showed that the β5i protein was efficiently precipitated by an antibody against ATG5 in the retina but not by a nonspecific immunoglobulin G (IgG) control (Fig. 5B). Thus, our results show that β5i directly interacts with ATG5, a finding that is also consistent with our previous results in cardiac hypertrophy.[12] In addition, we found that AKT and ERK1/2 were phosphorylated in WT OIR mice and that this phosphorylation was obviously attenuated in β5i KO OIR mice. VEGF was also significantly downregulated in β5i KO OIR mice compared with WT OIR mice (Fig. 5A), which means that pathological RNV is improved through autophagy activation followed by the AKT and ERK1/2 signaling pathways in β5i-deficient mice. Overall, these data demonstrate that β5i functionally links the immunoproteasome and autophagy by directly interacting with ATG5 and then modulates the pathologic process of RNV through the AKT and ERK1/2 signaling pathways (Fig. 5C).

Investigative Ophthalmology & Visual Science

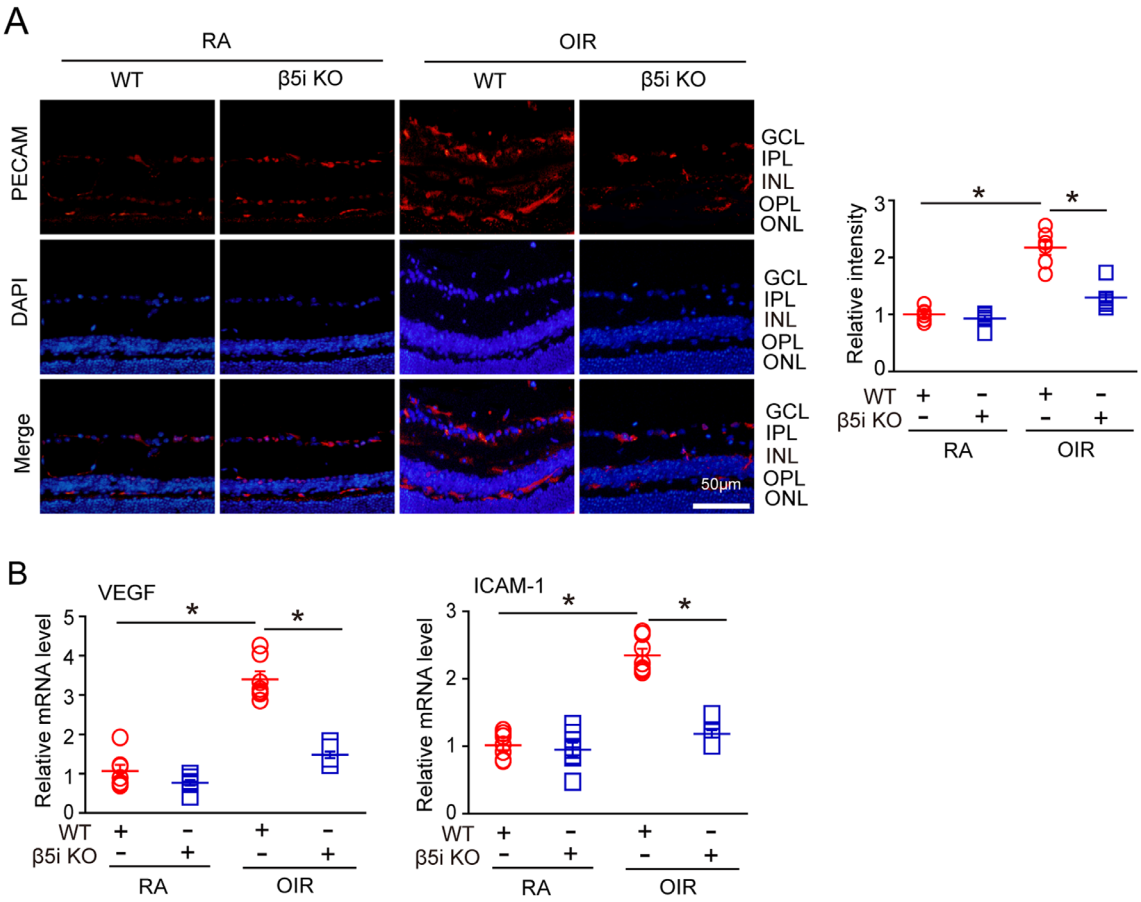

Figure 3. Genetic ablation of $\beta5$ reduces retinal endothelial related factors. (**A**) Immunostaining for PECAM, an endothelial marker, in retinal sections (*left*) from P17 mice and quantification of the relative fluorescence intensity (*right*) ($n = 6$ per group). (**B**) qPCR analysis of VEGF and ICAM-1 mRNA expression in retinas from P17 mice ($n = 7$ per group). All data are presented as mean ± SEM. $^{*}P < 0.05$ versus WT normoxia controls. *Scale bar*: 50 μm.

Discussion

Emerging evidence has indicated that the protein degradation system plays a role in modulating neovascularization.[29] In the present study, we addressed the specific role of $\beta5$i, an immunosubunit of the immunoproteasome, in pathologic RNV in a mouse model of OIR using $\beta5$i KO mice. Deletion of $\beta5$i significantly attenuated pathologic RNV, suggesting that $\beta5$i acts as a proangiogenic immunosubunit. We also found that $\beta5$i regulated autophagy by targeting ATG5, a central regulator of autophagy. These findings strongly indicate that $\beta5$i is a potential therapeutic target for RNV and acts as a bridge linking the immunoproteasome and autophagy in retinas with pathologic neovascularization.

It has been suggested that the UPS participates in almost all biological processes in eukaryotic cells.[11] In the ocular disease field, the UPS has been proposed to play a role in age-related macular degeneration,[30] diabetic retinopathy,[31,32] and retinitis pigmentosa.[33] As one of the major components of the UPS, the immunoproteasome plays a key role in antigen presentation, differentiation promotion, and immune cell regulation.[11] In addition, the immunoproteasome has been shown to be involved in ocular diseases, including hypertensive retinopathy and glaucoma.[14,15,22] Furthermore, an increasing number of studies has shown that $\beta1$i, $\beta2$i, and $\beta5$i are expressed in human, mouse, and rat retinas, including the GCL, IPL, and OPL.[34] $\beta1$i and $\beta5$i are increased in retinal injury[35]; however, limited studies have explored their functions in the pathologic process of RNV. Thus, we ran an OIR model that mimics in vivo pathologic RNV conditions. Our results definitively showed that $\beta5$i was the most upregulated immunosubunit and that chymotrypsin-like activity was also significantly induced, which indicated that, among immunoproteasome subunits, $\beta5$i was the greatest contributor to pathologic RNV formation. Based on this finding, we focused on exploring the role of $\beta5$i in pathologic RNV generation. Upregulation of $\beta5$i was further confirmed by immunofluorescence and immunoblotting in WT OIR mice. These results seem reasonable given that $\beta5$i might be involved in pathologic RNV.

Our approach to identifying the role of $\beta5$i was to utilize $\beta5$i KO mice. H&E staining confirmed that $\beta5$i deletion did not affect retinal histological features or structure. Notably, $\beta5$i deficiency reduced new retinal vessel generation, retinal avascular area, retinal vein width, and retinal artery tortuosity, in addition to downregulating neovascular-associated factors. Notably, $\beta5$i deletion resulted in less retinal central avascular area at P12, indicating that $\beta5$i deficiency inhibited the vaso-obliteration phase, resulting in less pathologic retinal neovascularization. Together, these findings indicate that $\beta5$i might be a potential therapeutic target for pathologic RNV.

Investigative Ophthalmology & Visual Science

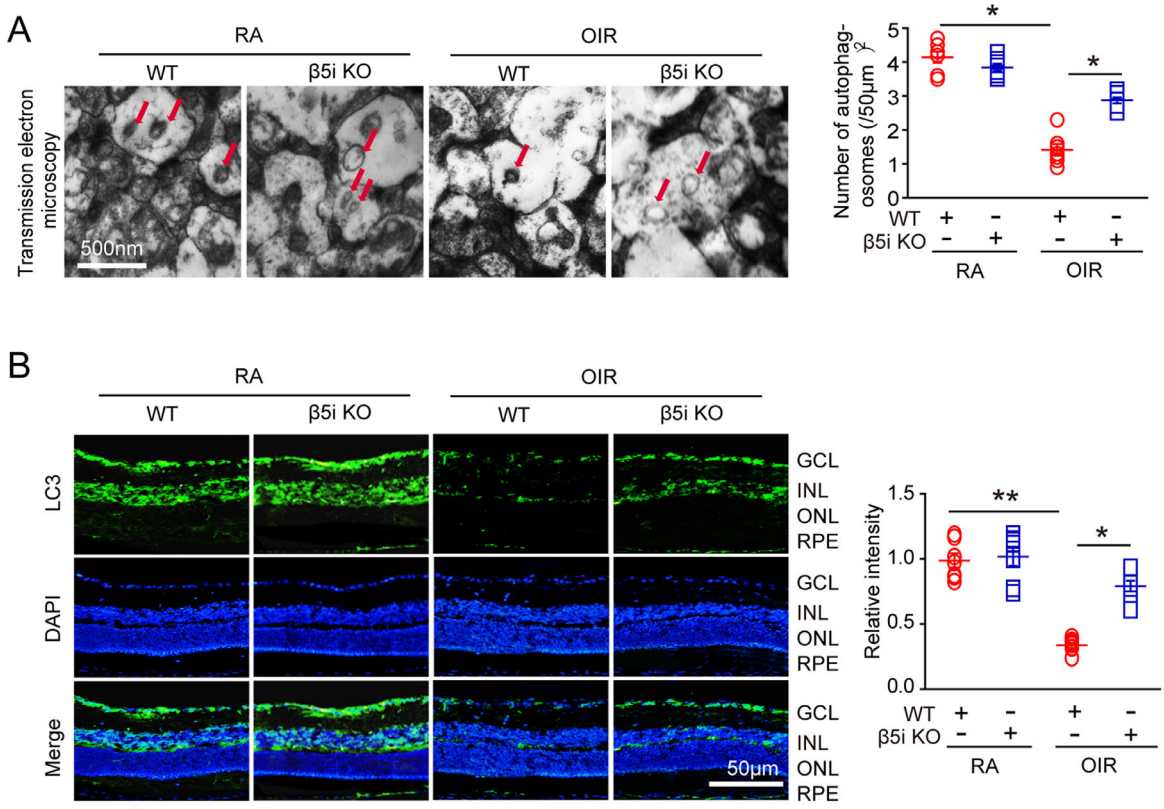

Figure 4. Autophagy is restored in the absence of β5i. (**A**) WT and β5i KO mice were placed in an oxygen chamber (75 ± 5% O_2) for 5 days beginning on P7 and then exposed to room air for another 5 days. Representative TEM images of the retina from P17 mice (*left*) (*red arrows* indicate autophagosomes) and quantification of the number of autophagosomes per 50-μm2 field (*right*) ($n = 7$ per group). (**B**) Representative images of LC3 immunostaining in retinal sections from P17 mice (*green* indicates LC3 and *blue* indicates DAPI) (*left*); quantification of the relative LC3 fluorescence intensity (*right*) ($n = 7$ per group). *Scale bars*: 50 μm.

Unlike the proteasomal system, which digests only short-lived cellular proteins, autophagy targets long-lived proteins to maintain cellular homeostasis.[9] Autophagy remains at baseline levels under normal conditions and can be regulated upon stimulation, such as inflammation and hypoxia.[16] Studies have shown that autophagy protects photoreceptors from death[36,37] and enhances retinal ganglion cell survival in glaucoma and ischemia.[38] Specific genes, including ATG5, ATG6, and ATG7, are responsible for modulating autophagy.[16] Among these genes, ATG5 is a central molecule involved in autophagy elongation. The conjugation system of autophagy involves ATG7, ATG10, and ATG16L1, which form the multimeric ATG5–ATG12–ATG16L1 complex.[39] This complex is essential for converting LC3-I to LC3-II.[39] Our previous study revealed that autophagy is attenuated in pathologic RNV[6]; however, the underlying mechanisms still must be explored. Recently, studies have shown that there is a complementary relationship between autophagy and the immunoproteasome.[18,40,41] A previous report has shown that NDP52, an autophagy receptor, links autophagy and the UPS.[42] Rapamycin-induced autophagy promotes cell survival in the presence of proteasome inhibitors in vivo and in vitro.[43,44] Proteasome inhibition activates autophagy, with p62 acting as a bridge.[45,46] To confirm whether this complementary relationship occurs in pathologic RNV, autophagy changes were investigated in the absence of immunosubunit β5i. Our findings clearly demonstrate that autophagy was decreased in WT OIR mice compared to WT mice but dramatically increased in β5i KO OIR mice. This finding specifically supports a correlation between the immunoproteasome and autophagy.

To gain further insight into how these two degradation systems are linked, central initiators of autophagy were examined. Our findings indicate that ATG5 showed opposite changes in the presence and absence of β5i. Based on our results, we speculated that ATG5 might directly interact with β5i. As expected, β5i was precipitated by an anti-ATG5 antibody but not by control IgG, which further confirmed our speculation. These findings comprehensively indicate that autophagy was restored by stabilization of ATG5 when β5i was knocked out, which strongly supports the complementary effects of the immunoproteasome and autophagy. To uncover the underlying mechanism of improvements in pathologic RNV, signaling pathways were evaluated. The phosphorylation of AKT and ERK1/2 in β5i KO mice was reduced compared with that in WT OIR mice. Our findings clearly show that β5i deletion improves pathologic RNV through inhibiting AKT and ERK signaling pathways, thus further downregulating VEGF secretion (Fig. 5C). Further studies are needed to evaluate the potential therapeutic role of in vivo neutralization of β5i in pathologic RNV.

To conclude, we discovered that β5i is a proangiogenic immunosubunit and documented its functional role in modulating pathological RNV. Ablation of β5i stabilizes ATG5, restores autophagy, and further ameliorates pathological RNV through the AKT and ERK1/2 signaling pathways. This indicates a critical role of β5i in linking the immunoproteasome and autophagy; therefore, β5i

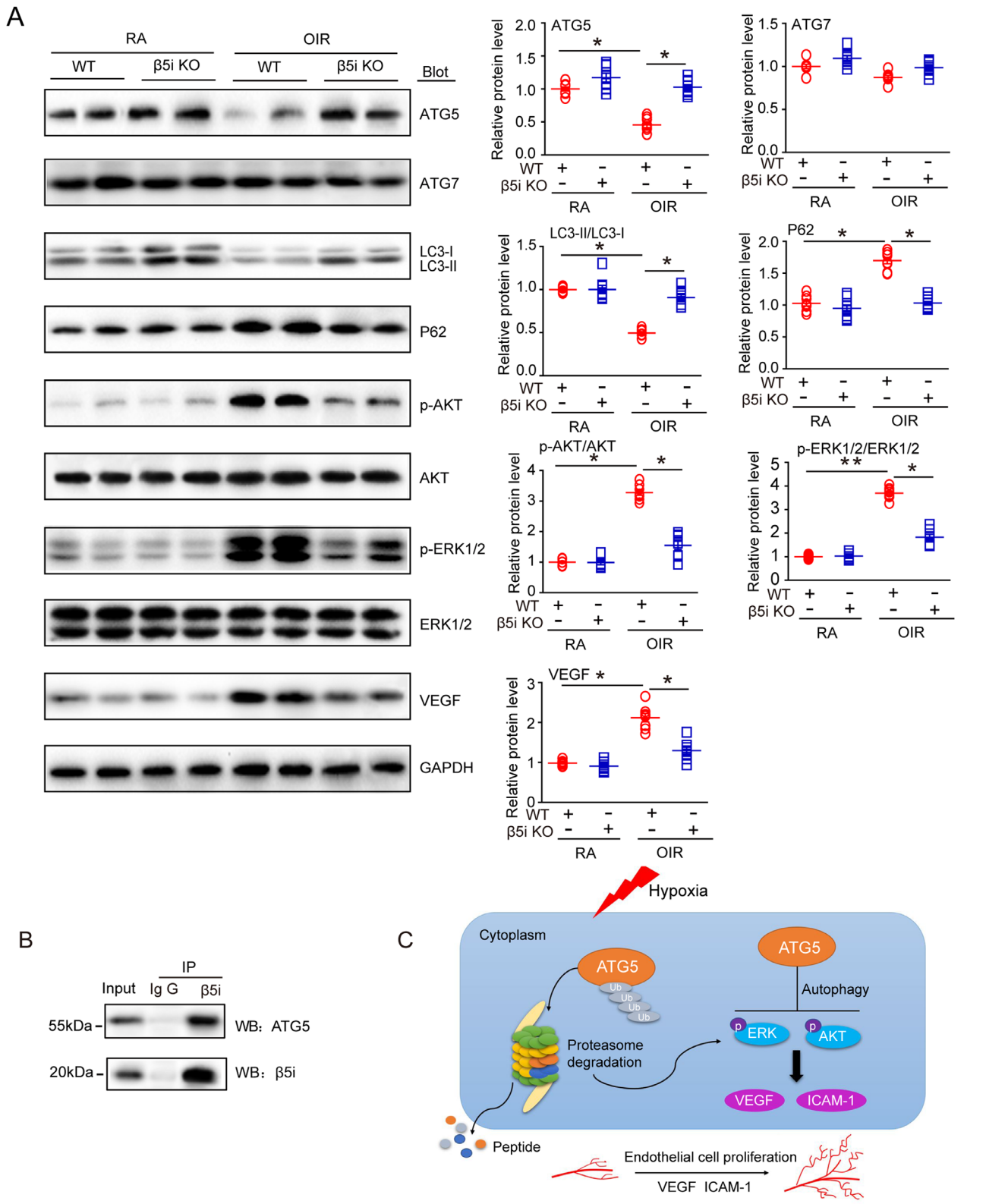

Figure 5. β5i regulates autophagy by directly targeting ATG5. (**A**) WT and β5i KO mice were placed in an oxygen chamber (75 ± 5% O_2) for 5 days beginning on P7 and then exposed to room air for another 5 days. Representative images of immunoblotting analysis of β5i, ATG5, ATG7, LC3, P62, p-AKT, AKT, p-ERK1/2, ERK1/2, VEGF, and GAPDH protein in the retinas from P17 mice (*left*) and quantification after normalization to GAPDH (*right*) ($n = 8$ per group). (**B**) Endogenous protein interactions were examined in P17 retinal lysates immunoprecipitated with rabbit IgG or an anti-β5i antibody and analyzed by western blotting with antibodies against ATG5 and β5i. (**C**) A working model of the mechanism by which β5i modulates pathologic RNV. After β5i deletion, ATG5 avoids degradation and restores autophagy, resulting in downregulation of the p-AKT and p-ERK signaling pathways, as well as reduced pathologic RNV.

Investigative Ophthalmology & Visual Science

might be a potential therapeutic target for pathologic RNV treatment.

Acknowledgments

The authors thank Huihua Li for kindly sharing β5i KO mice and all reviewers for their valuable comments.

Supported by Grants from the National Natural Science Foundation of China (81900880) and Natural Foundation of Liaoning Province (20180550740), and by Joint Fund of Collaborative Innovation Center for Individualized Diagnosis and Treatment (dy2yhws201804).

Disclosure: **L. Ji**, None; **L. Li**, None; **Y. Zhao**, None; **S. Liu**, None; **J. Li**, None; **J. Zhang**, None; **Q. Zhao**, None; **S. Wang**, None

References

1. Kusuhara S, Fukushima Y, Ogura S, Inoue N, Uemura A. Pathophysiology of diabetic retinopathy: the old and the new. *Diabetes Metab J*. 2018;42(5):364–376.
2. Patel A, Nguyen C, Lu S. Central retinal vein occlusion: a review of current evidence-based treatment options. *Middle East Afr J Ophthalmol*. 2016;23(1):44–48.
3. Campochiaro PA. Molecular pathogenesis of retinal and choroidal vascular diseases. *Prog Retin Eye Res*. 2015;49:67–81.
4. Campochiaro PA. Retinal and choroidal neovascularization. *J Cell Physiol*. 2000;184(3):301–310.
5. Rivera JC, Madaan A, Zhou TE, Chemtob S. Review of the mechanisms and therapeutic avenues for retinal and choroidal vascular dysfunctions in retinopathy of prematurity. *Acta Paediatr*. 2016;105(12):1421–1433.
6. Wang S, Ji LY, Li L, Li JM. Oxidative stress, autophagy and pyroptosis in the neovascularization of oxygen-induced retinopathy in mice. *Mol Med Rep*. 2019;19(2):927–934.
7. Zhang SX, Ma JH, Bhatta M, Fliesler SJ, Wang JJ. The unfolded protein response in retinal vascular diseases: implications and therapeutic potential beyond protein folding. *Prog Retin Eye Res*. 2015;45:111–131.
8. Rivera JC, Dabouz R, Noueihed B, Omri S, Tahiri H, Chemtob S. Ischemic retinopathies: oxidative stress and inflammation. *Oxid Med Cell Longev*. 2017;2017:3940241.
9. Wang Y, Le WD. Autophagy and ubiquitin-proteasome system. *Adv Exp Med Biol*. 2019;1206:527–550.
10. Ferrington DA, Gregerson DS. Immunoproteasomes: structure, function, and antigen presentation. *Prog Mol Biol Transl Sci*. 2012;109:75–112.
11. Murata S, Takahama Y, Kasahara M, Tanaka K. The immunoproteasome and thymoproteasome: functions, evolution and human disease. *Nat Immunol*. 2018;19(9):923–931.
12. Xie X, Bi HL, Lai S, et al. The immunoproteasome catalytic β5i subunit regulates cardiac hypertrophy by targeting the autophagy protein ATG5 for degradation. *Sci Adv*. 2019;5(5):eaau0495.
13. Hussong SA, Kapphahn RJ, Phillips SL, Maldonado M, Ferrington DA. Immunoproteasome deficiency alters retinal proteasome's response to stress. *J Neurochem*. 2010;113(6):1481–1490.
14. Ying H, Turturro S, Nguyen T, et al. Induction of autophagy in rats upon overexpression of wild-type and mutant optineurin gene. *BMC Cell Biol*. 2015;16:14.
15. Wang S, Li J, Wang T, et al. Ablation of immunoproteasome β5i subunit suppresses hypertensive retinopathy by blocking ATRAP degradation in mice. *Mol Ther*. 2020;28(1):279–292.
16. Ravanan P, Srikumar IF, Talwar P. Autophagy: the spotlight for cellular stress responses. *Life Sci*. 2017;188:53–67.
17. Shen X, Ying H, Qiu Y, et al. Processing of optineurin in neuronal cells. *J Biol Chem*. 2011;286(5):3618–3629.
18. Nedelsky NB, Todd PK, Taylor JP. Autophagy and the ubiquitin-proteasome system: collaborators in neuroprotection. *Biochim Biophys Acta*. 2008;1782(12):691–699.
19. Smith LE, Wesolowski E, McLellan A, et al. Oxygen-induced retinopathy in the mouse. *Invest Ophthalmol Vis Sci*. 1994;35(1):101–111.
20. Kilkenny C, Browne WJ, Cuthill IC, Emerson M, Altman DG. Improving bioscience research reporting: the ARRIVE guidelines for reporting animal research. *Osteoarthritis Cartilage*. 2012;20(4):256–260.
21. McGill TJ, Prusky GT, Luna G, LaVail MM, Fisher SK, Lewis GP. Optomotor and immunohistochemical changes in the juvenile S334ter rat. *Exp Eye Res*. 2012;104:65–73.
22. Wang S, Li J, Bai J, et al. The immunoproteasome subunit LMP10 mediates angiotensin II-induced retinopathy in mice. *Redox Biol*. 2018;16:129–138.
23. Mezu-Ndubuisi OJ. In vivo angiography quantifies oxygen-induced retinopathy vascular recovery. *Optom Vis Sci*. 2016;93(10):1268–1279.
24. Mezu-Ndubuisi OJ, Teng PY, Wanek J, et al. In vivo retinal vascular oxygen tension imaging and fluorescein angiography in the mouse model of oxygen-induced retinopathy. *Invest Ophthalmol Vis Sci*. 2013;54(10):6968–6972.
25. Tawfik A, Markand S, Al-Shabrawey M, et al. Alterations of retinal vasculature in cystathionine-beta-synthase heterozygous mice: a model of mild to moderate hyperhomocysteinemia. *Am J Pathol*. 2014;184(9):2573–2585.
26. Livak KJ, Schmittgen TD. Analysis of relative gene expression data using real-time quantitative PCR and the 2(-Delta Delta C(T)) method. *Methods*. 2001;25(4):402–408.
27. Banin E, Dorrell MI, Aguilar E, et al. T2-TrpRS inhibits preretinal neovascularization and enhances physiological vascular regrowth in OIR as assessed by a new method of quantification. *Invest Ophthalmol Vis Sci*. 2006;47(5):2125–2134.
28. Martini D, Monte MD, Ristori C, et al. Antiangiogenic effects of β2-adrenergic receptor blockade in a mouse model of oxygen-induced retinopathy. *J Neurochem*. 2011;119(6):1317–1329.
29. Lee JY, Park JH, Choi HJ, et al. LSD1 demethylates HIF1α to inhibit hydroxylation and ubiquitin-mediated degradation in tumor angiogenesis. *Oncogene*. 2017;36(39):5512–5521.
30. Fernandes AF, Bian Q, Jiang JK, et al. Proteasome inactivation promotes p38 mitogen-activated protein kinase-dependent phosphatidylinositol 3-kinase activation and increases interleukin-8 production in retinal pigment epithelial cells. *Mol Biol Cell*. 2009;20(16):3690–3699.
31. Ozawa Y, Kurihara T, Sasaki M, et al. Neural degeneration in the retina of the streptozotocin-induced type 1 diabetes model. *Exp Diabetes Res*. 2011;2011:108328.
32. Ozawa Y, Kurihara T, Tsubota K, Okano H. Regulation of posttranscriptional modification as a possible therapeutic approach for retinal neuroprotection. *J Ophthalmol*. 2011;2011:506137.
33. Friedman JS, Ray JW, Waseem N, et al. Mutations in a BTB-Kelch protein, KLHL7, cause autosomal-dominant retinitis pigmentosa. *Am J Hum Genet*. 2009;84(6):792–800.
34. Campello L, Esteve-Rudd J, Cuenca N, Martin-Nieto J. The ubiquitin-proteasome system in retinal health and disease. *Mol Neurobiol*. 2013;47(2):790–810.

35. Ferrington DA, Hussong SA, Roehrich H, et al. Immunoproteasome responds to injury in the retina and brain. *J Neurochem*. 2008;106(1):158–169.
36. Rodriguez-Muela N, Hernandez-Pinto AM, Serrano-Puebla A, et al. Lysosomal membrane permeabilization and autophagy blockade contribute to photoreceptor cell death in a mouse model of retinitis pigmentosa. *Cell Death Differ*. 2015;22(3):476–487.
37. Chen Y, Sawada O, Kohno H, et al. Autophagy protects the retina from light-induced degeneration. *J Biol Chem*. 2013;288(11):7506–7518.
38. Lin WJ, Kuang HY. Oxidative stress induces autophagy in response to multiple noxious stimuli in retinal ganglion cells. *Autophagy*. 2014;10(10):1692–1701.
39. Otomo C, Metlagel Z, Takaesu G, Otomo T. Structure of the human ATG12~ATG5 conjugate required for LC3 lipidation in autophagy. *Nat Struct Mol Biol*. 2013;20(1):59–66.
40. Korolchuk VI, Menzies FM, Rubinsztein DC. Mechanisms of cross-talk between the ubiquitin-proteasome and autophagy-lysosome systems. *FEBS Lett*. 2010;584(7):1393–1398.
41. Pandey UB, Nie Z, Batlevi Y, et al. HDAC6 rescues neurodegeneration and provides an essential link between autophagy and the UPS. *Nature*. 2007;447(7146):859–863.
42. Fan S, Wu K, Zhao M, et al. The role of autophagy and autophagy receptor NDP52 in microbial infections. *Int J Mol Sci*. 2020;21(6):2008.
43. Russo R, Varano GP, Adornetto A, et al. Rapamycin and fasting sustain autophagy response activated by ischemia/reperfusion injury and promote retinal ganglion cell survival. *Cell Death Dis*. 2018;9(10):981.
44. Guo F, He XB, Li S, Le W. A central role for phosphorylated p38α in linking proteasome inhibition-induced apoptosis and autophagy. *Mol Neurobiol*. 2017;54(10):7597–7609.
45. Tang B, Cai J, Sun L, et al. Proteasome inhibitors activate autophagy involving inhibition of PI3K-Akt-mTOR pathway as an anti-oxidation defense in human RPE cells. *PLoS One*. 2014;9(7):e103364.
46. Cortes CJ, La Spada AR. Autophagy in polyglutamine disease: imposing order on disorder or contributing to the chaos? *Mol Cell Neurosci*. 2015;66(pt A):53–61.